Origin of superconductivity in boron-doped silicon carbide from first principles

Jesse Noffsinger, Feliciano Giustino, Steven G. Louie, and Marvin L. Cohen

Department of Physics, University of California-Berkeley, Berkeley, California 94720, USA

and Materials Sciences Division, Lawrence Berkeley National Laboratory, Berkeley, California 94720, USA

We investigate the origin of superconductivity in boron-doped silicon carbide using a first-principles approach. The strength of the electron-phonon coupling calculated for cubic SiC at the experimental doping level suggests that the superconductivity observed in this material is phonon mediated. Analysis of the 2*H*-SiC, 4*H*-SiC, 6*H*-SiC, and 3*C*-SiC polytypes indicates that superconductivity depends on the stacking of the Si and C layers and that the cubic polytype will exhibit the highest transition temperature. In contrast to the cases of silicon and diamond, acoustic phonons are found to play a major role in the superconductivity of silicon carbide.

Silicon carbide is a promising material for a variety of emerging applications. Its large band gap, high breakdown field, and high melting point make it ideal for uses in high-power devices, radiation tolerant electronics,[1] and optoelectronics.[2] Besides its widespread use in devices for harsh environments, SiC has also proven to be a promising biocompatible material, with potential uses in implantable sensors.[3]

Recently, B-doped samples of 3*C*-SiC were reported to superconduct at 1.4 K.[4] The superconducting properties of semiconductors were predicted several decades ago,[5] and the discovery of superconductivity in boron-doped diamond[6] and silicon[7] sparked significant interest in this research area. The critical temperature of doped diamond has been raised above 11 K since the original discovery.[8] However, diamond-based devices are still impractical for applications.[9] On the other hand, although silicon electronics benefits from a well-established industrial infrastructure, B-doped silicon undergoes a phase transition to the superconducting state at the very low temperature of 0.3 K, and the gas immersion laser method used to achieve the required levels of doping is a challenging technique.[7] Within this framework, silicon carbide stands as a promising compromise between the former two materials: (i) the infrastructure for producing SiC is already well established, and (ii) boron doping can be achieved without major difficulties.

In this work we investigate from first principles the origin of superconductivity in boron-doped silicon carbide. First, we study the electron-phonon coupling strength in the cubic polytype 3*C* of silicon carbide by simulating the hole doping through a rigid-band (RB) model. Then, we consider the electron-phonon interaction in a supercell (SC) model of the 3*C*-SiC to validate our results. Finally, we determine the relative strength of the electron-phonon coupling in different polytypes of silicon carbide. Our investigation indicates that the total coupling strength ranges from $\lambda = 0.21$ to $\lambda = 0.34$ among all polytypes considered. Using the McMillan equation with Coulomb parameter $\mu^* = 0.1$,[10] we obtain superconducting transition temperatures between 0.01 and 1.1 K, in good accord with experimental data.

SiC polytypes consist of tetrahedrally bonded silicon and carbon atoms. The structural difference among the polytypes results from the stacking of the silicon-carbon tetrahedra

along the *c* axis. For example, the stacking in 2*H*-SiC corresponds to a periodicity of two layers of Si and C (*AB*), while the stacking in 6*H*-SiC corresponds to a periodicity of six layers (*ABCACB*). In this work we first discuss the cubic polytype 3*C*-SiC because the superconducting samples in the experiment of Ref. 4 were reported to be primarily of the 3*C* type. We then extend our investigation to the 4*H*-SiC and the 6*H*-SiC polytypes which are important for device applications.[11,12]

In the original experiment of Ref. 4, 3*C*-SiC samples were synthesized with a 4% concentration of boron. Structural analysis indicated that B dopants substitutionally replaced the C atoms. In our calculations we considered two distinct doping levels. First, we studied 3*C*-SiC with a realistic boron concentration of 3.7%. In this case we explore both a rigid-band model (for the electronic structure, the lattice dynamics, and the electron-phonon interaction: model I-RB in the following) and a $3 \times 3 \times 3$ supercell model (for the electronic structure: model I-SC). Then, we studied 3*C*-SiC with a B concentration of 12.5%, substantially larger than in the original experiment.[4] In this latter case we compared again a rigid-band model (model II-RB) with a $2 \times 2 \times 2$ supercell model (for which we studied the electronic structure, the lattice dynamics, and the electron-phonon coupling: model II-SC). The calculations for the other polytypes were all performed within the rigid-band approximation. We described the electronic structure using the local density approximation[13,14] to density-functional theory, within a plane-wave pseudopotential scheme.[15–17] We calculated the lattice dynamical properties using density-functional perturbation theory,[18] and the electron-phonon coupling parameter using an interpolation scheme[19] based on maximally localized Wannier functions.[20–22]

Figure 1 shows a comparison between the band structures of 3.7% B-doped 3*C*-SiC calculated within the rigid-band model, I-RB, and within the supercell model, I-SC. In both cases, the doping has the effect of lowering the Fermi level below the top of the valence band. As a result, a small multisheet Fermi surface emerges around the center of the Brillouin zone. Importantly, the dopants do not introduce localized states in the band gap. The close similarity between the electronic bands of model I-RB and model I-SC around the Fermi level provides a justification for the use of the rigid-
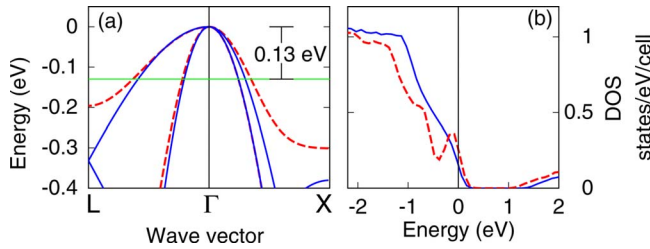
FIG. 1. (Color online) (a) Band structure of 3.7% B-doped 3*C*-SiC: model I-RB (solid blue lines) and model I-SC (dashed red lines). The zero of energy is set to the top of the valence bands, and the Fermi level is indicated by the horizontal line. (b) Electronic density of 3.7% B-doped 3*C*-SiC: model I-RB (solid blue line) and model I-SC (dashed red line). The density of states at the Fermi level is similar in the two models (0.18 states/eV/cell in model I-RB and 0.23 states/eV/cell in model I-SC). In the supercell model we do not find impurity states within the band gap.

band approximation to describe the electronic structure of B-doped SiC. This finding is analogous to what had already been observed in the case of B-doped diamond.[23,24] Our results are consistent with previous experimental work on SiC showing that the Mott metal-to-insulator transition occurs at a hole-doping concentration of 10^{21} cm^{-3}.[25] In fact, the dopant concentration considered here, corresponding to a hole concentration of 2×10^{21} cm^{-3}, clearly lies within the metallic regime, consistent with Fig. 1.

Figure 2 shows the phonon dispersions calculated for pristine and for hole-doped 3*C*-SiC. In the case of pristine 3*C*-SiC, the calculated phonon dispersions are in good agreement with the experimental data of Ref. 26. In particular, we find a splitting of 23 meV between the longitudinal optical (LO) and the transverse optical (TO) phonons at the Γ point, in accord with the measured value of 21 meV. In order to discuss the lattice dynamics of B-doped SiC, we first present our results for model I-RB and then extend our discussion using models II-RB and II-SC. In model I-RB, upon doping the LO-TO splitting is closed by the metallic screening and the optical phonons become degenerate at the zone center. From pristine to hole-doped SiC the TO mode at Γ is softened by 5.5 meV and the LO mode by 26.5 meV, similar to the cases of boron-doped diamond[27] and silicon.[7] The dispersions throughout the rest of the Brillouin zone are only weakly affected by the doping. This is also similar to the case of boron-doped diamond where the optical phonons are softened only if their wave vector is smaller than $\sim 2k_F$ (k_F is the average radius of the Fermi surface in reciprocal space).[24,28] In Refs. 23 and 24 it was pointed out that B-doped diamond exhibits partially localized vibrational modes associated with the dopant. These modes give rise to a nondispersive feature below the optical branches[24] and cannot be described by a rigid-band model. In order to check for the existence of those modes in the case of SiC, we unfolded the phonon dispersions of supercell model II-SC into the Brillouin zone of pristine SiC following Ref. 24. Figure 2 indicates that the acoustic modes of the II-RB and II-SC models align closely. The branch splitting at zone edges arises from the impurity potential in the heavily doped supercell. As in the case of boron-doped diamond, the optical
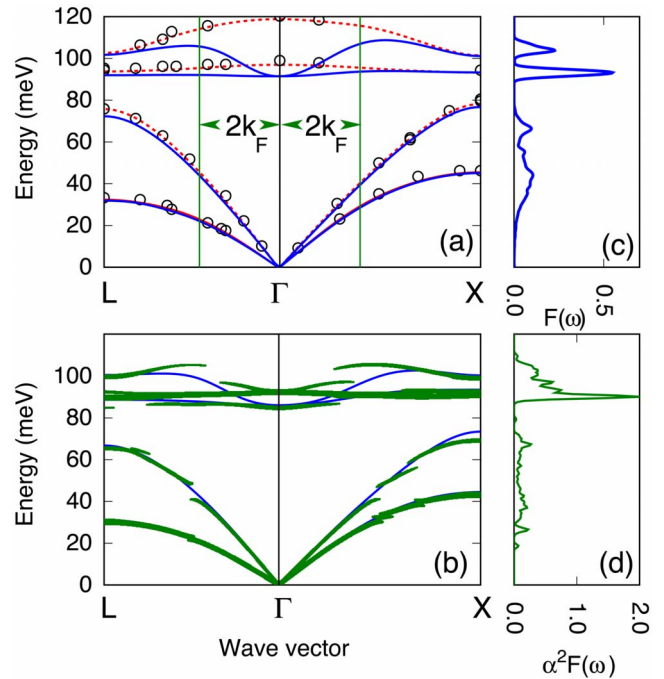

FIG. 2. (Color online) (a) Phonon dispersions of pristine (dashed red lines) and B-doped (solid blue lines) 3*C*-SiC along the Λ and the Δ directions of the Brillouin zone. The vertical (green) lines indicate the average Fermi surface diameter. Open circles are experimental data (Ref. 26). (b) Phonon dispersions for heavily B-doped 3*C*-SiC: model II-RB (solid blue lines) and model II-SC (green points, after folding into the Brillouin zone of pristine SiC, following Ref. 24). (c) Phonon density of states for model I-RB. (d) The Eliashberg spectral function for 12.5% B-doped 3*C*-SiC (model II-SC). The nondispersive branch around 80 meV in (b) does not contribute to the Eliashberg spectral function.

modes exhibit a nondispersive feature below the optical branches, which is associated with localized motion around the boron atoms. However, in contrast to the case of B-doped diamond, the impurity branch has negligible contribution to the total electron-phonon coupling [cf. the Eliashberg spectral function in Fig. 2(d)]. This finding indicates that a rigid-band model is appropriate to describe the electron-phonon interaction in B-doped SiC.

Figure 3 shows the Eliashberg spectral function $\alpha^2 F(\omega)$ for model I-RB, calculated using Eq. (7) of Ref. 19. The Eliashberg function exhibits two sharp peaks at the energies of 92 and 106 meV, associated with the Van Hove singularities in the phonon dispersion relations (cf. Fig. 2). In addition to the optical peaks, a broad, although less-pronounced, feature appears in the acoustic energy range. Interestingly, the coupling of electrons to the acoustic phonons is negligible above 40 meV despite the nonvanishing vibrational density of states [Fig. 2(c)]. This can be understood by considering that the wave vector of acoustic phonons with energy in excess of 40 meV is larger than $\sim 2k_F$ [cf. Fig. 2(a)]; hence, they cannot promote electronic transitions within the Fermi surface. At variance with this finding, in the heavily doped case (model II-SC) there is some noticeable contribution of high-energy acoustic phonons to the Eliashberg function, corresponding to a wider Fermi surface [Fig. 2(d)].
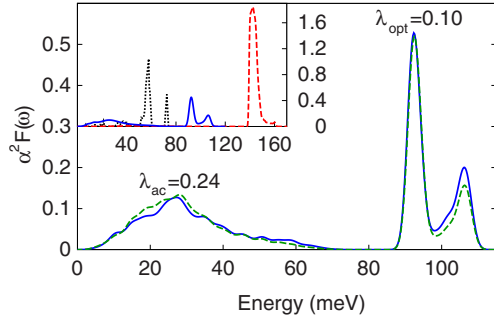
FIG. 3. (Color online) Eliashberg function $\alpha^2F(\omega)$ for model I-RB of 3.7% B-doped 3C-SiC (solid blue line). We also show the Eliashberg function obtained using a constant electron-phonon matrix element g=95 meV for comparison (dashed green line). (Inset) Comparison between the Eliashberg functions of B-doped SiC (solid blue line, model I-RB), diamond (dashed red line, from Ref. 24), and silicon (dotted black line, from Ref. 29). The contribution of the acoustic phonons to the electron-phonon coupling parameter is significant in SiC, whereas it is small or negligible in diamond and silicon.

The first reciprocal energy moment of the Eliashberg spectral function provides the electron-phonon coupling parameter $\lambda=2\int\omega^{-1}\alpha^2F(\omega)$. For model I-RB of 3.7% B-doped 3C-SiC we find a coupling parameter of λ=0.34. The coupling of the electrons to the acoustic phonons accounts for 70% of the total coupling strength. This result is qualitatively different from the cases of B-doped diamond and silicon, where the coupling to the acoustic modes accounts for less than 25% of the total electron-phonon coupling strength, as found by integrating the spectral functions of Refs. 24 and 29. Furthermore, we find that the Eliashberg function of B-doped 3C-SiC can be reproduced quite accurately by taking the electron-phonon matrix element g constant and equal to 95 meV (dashed line in Fig. 3). This indicates that superconductivity in SiC is dominated by the geometry of the Fermi surface and by the vibrational density of states, as opposed to the coupling of electrons to specific vibrational modes as is the case in diamond.[23,24] A band-by-band decomposition of the coupling parameter reveals indeed that intraband scattering processes within the largest Fermi surface of 3C-SiC (Ref. 30) are favored by the peculiar nesting features of this surface and provide the dominant contribution to the pairing. This mechanism has not been observed for B-doped diamond.[31]

The superconducting transition temperature corresponding to the calculated electron-phonon coupling parameter is obtained using the modified McMillan equation.[10] The average logarithmic phonon frequency [Eq. (14.2) of Ref. 32] is ω_{log}=63 meV, considerably smaller than the one calculated for B-doped diamond in Ref. 24 (125 meV). The relatively small logarithmic frequency results from the large contribution of the acoustic phonons in SiC, which enhances the weight of the Eliashberg function in the low-frequency range. Depending on the choice of the Coulomb parameter μ^*, the calculated superconducting transition temperature varies between 0.09 (μ^*=0.15) and 1.1 K (μ^*=0.1). The latter value compares favorably with the measured transition temperature of 1.4 K. These results indicate that the experi-

TABLE I. Electron-phonon interaction strength in various polytypes of 3.7% doped SiC. We show the total coupling strength (λ_{tot}), as well as the contributions arising from the acoustic (λ_{ac}) and the optical (λ_{opt}) phonons. The superconducting transition temperature (T_c in kelvin) is estimated using the McMillan formula with a Coulomb parameter μ^*=0.1. The calculations on the hexagonal polytypes have been performed using a rigid-band model. The accuracy in the calculated coupling parameters λ_{tot} is the same across different polytypes, while the T_c values depend exponentially on λ_{tot} and are shown purely for comparison purposes.

	3C	2H	4H	6H
λ_{ac}	0.24	0.15	0.12	0.14
λ_{opt}	0.10	0.09	0.09	0.07
λ_{tot}	0.34	0.24	0.21	0.21
T_c (K)	1	0.01	0.001	0.001

mentally observed superconductivity in SiC can be explained with an electron-phonon coupling mechanism.

In order to validate our results based on the rigid-band model I-RB, we performed additional calculations for the heavily doped rigid-band (II-RB) and supercell (II-SC) models of B-doped SiC. In these latter models we consider a very large boron concentration of 12.5% (not yet achieved in experiment) in order to compare the rigid-band approach and the supercell approach in a limiting situation The electron-phonon coupling parameter was found to be λ_{II-RB}=0.44 for model II-RB and λ_{II-SC}=0.46 for model II-SC. Inspection of the Eliashberg function for models II-RB and II-SC reveals no significant differences in the sources of coupling for these two models. The close agreement between the rigid-band and the supercell calculations provides an *a posteriori* justification for our choice of modeling 3.7% B-doped 3C-SiC within a rigid-band approximation. Interestingly, the superconducting transition temperatures of heavily doped models II-RB (5.1 K for μ^*=0.1) and II-SC (6.3 K for μ^*=0.1) are found to be above the boiling point of liquid helium. This result bears potential implications for practical uses of superconducting SiC.

After discussing the mechanism of superconductivity in 3C-SiC, we now extend our investigation to the 4H-SiC and 6H-SiC polytypes which are of interest for applications and to the 2H-SiC polytype for completeness. For each of these polytypes the valence-band maximum occurs at the zone center, and the B doping gives rise to a multisheet Fermi surface around Γ of similar topology. Our calculations indicate that the electron-phonon coupling in polytypes 2H-SiC, 3C-SiC, 4H-SiC, and 6H-SiC occurs in the range of λ =0.21–0.34 for comparable levels of doping (Table I). The electron-phonon coupling strength associated with the optical modes is very similar for all of the polytypes (λ =0.07–0.10). This is consistent with the fact that optical phonons around the zone center correspond to bond-stretching vibrations which are sensitive to the short-range structure, which is the same in all polytypes. In contrast, the coupling to low-energy acoustic phonons exhibits a larger variation (λ=0.12–0.23) and is enhanced in 3C-SiC. We assign this variation to the differences in the shape of the Fermi

surfaces among the polytypes (some leading to a more pronounced nesting).

Recently, a metal-insulator transition has been observed in Al-doped SiC,[25] raising the question as to whether electron doping of SiC could be a more convenient strategy to increase its superconducting transition temperature. In order to address this question we have calculated the electron-phonon coupling parameter of Al-doped SiC within the rigid-band approximation. The coupling parameter is found to be smaller than in B-doped SiC for comparative levels of doping ($\lambda = 0.15$ for 5% Al doping and $\lambda = 0.29$ for 15% Al doping), indicating that hole doping is more advantageous in view of optimizing superconductivity in SiC.

In conclusion, we investigated the origin of superconductivity in boron-doped silicon carbide from first principles by considering a large set of structural models. We find that superconductivity arises from conventional phonon-mediated pairing. The transition temperature ranges from 1.1 (for a B concentration of 3.7%) to 6.3 K (12.5%). In contrast to the related B-doped Si and diamond systems, acoustic phonons and Fermi surface nesting play a prominent role in the superconductivity of SiC. Our study suggests that heavily doped cubic SiC may be a potential candidate for technological uses of superconducting semiconductors.

Note added. Recently, another theoretical work investigating the superconductivity in doped SiC was published.[35] Our results and conclusions are in agreement with those presented in that work.

[1] N. G. Wright, A. B. Horsfall, and K. Vassilevski, Mater. Today **11**, 16 (2008).

[2] W. J. Choyke, H. Matsunami, and G. Pensl, *Silicon Carbide: Recent Major Advances* (Springer-Verlag, Berlin, 2004).

[3] A. J. Rosenbloom, Y. Shishkin, D. M. Sipe, Y. Ke, R. P. Devaty, and W. J. Choyke, Mater. Sci. Forum **457-460**, 1463 (2004).

[4] Z.-A. Ren, J. Kato, T. Muranaka, J. Akimitsu, M. Kriener and Y. Maeno, J. Phys. Soc. Jpn. **76**, 103710 (2007).

[5] M. L. Cohen, Rev. Mod. Phys. **36**, 240 (1964).

[6] E. A. Ekimov, V. A. Sidorov, E. D. Bauer, N. N. Mel'nik, N. J. Curro, J. D. Thompson and S. M. Stishov, Nature (London) **428**, 542 (2004).

[7] E. Bustarret, C. Marcenat, P. Achatz, J. Kačmarčik, F. Lévy, A. Huxley, L. Ortéga, E. Bourgeois, X. Blase, D. Débarre, and J. Boulmer, Nature (London) **444**, 465 (2006).

[8] K. Ishizaka, R. Eguchi, S. Tsuda, T. Yokoya, A. Chainani, T. Kiss, T. Shimojima, T. Togashi, S. Watanabe, C. -T. Chen, C. Q. Zhang, Y. Takano, M. Nagao, I. Sakaguchi, T. Takenouchi, H. Kawarada, and S. Shin, Phys. Rev. Lett. **98**, 047003 (2007).

[9] C. J. H. Wort and R. S. Balmer, Mater. Today **11**, 22 (2008).

[10] P. B. Allen and R. C. Dynes, Phys. Rev. B **12**, 905 (1975).

[11] Q. Wahab, T. Kimoto, A. Ellison, C. Hallin, M. Tuominen, R. Yakimova, A. Henry, J. P. Bergman and E. Janzén, Appl. Phys. Lett. **72**, 445 (1998).

[12] L. G. Matus, J. A. Powell, and C. S. Salupo, Appl. Phys. Lett. **59**, 1770 (1991).

[13] D. M. Ceperley and B. J. Alder, Phys. Rev. Lett. **45**, 566 (1980).

[14] J. P. Perdew and A. Zunger, Phys. Rev. B **23**, 5048 (1981).

[15] J. Ihm, A. Zunger, and M. L. Cohen, J. Phys. C **12**, 4409 (1979).

[16] N. Troullier and J. L. Martins, Phys. Rev. B **43**, 1993 (1991).

[17] M. Fuchs and M. Scheffler, Comput. Phys. Commun. **119**, 67 (1999).

[18] S. Baroni, S. de Gironcoli, A. Dal Corso, and P. Gianozzi, Rev. Mod. Phys. **73**, 515 (2001).

[19] F. Giustino, M. L. Cohen, and S. G. Louie, Phys. Rev. B **76**, 165108 (2007).

[20] N. Marzari and D. Vanderbilt, Phys. Rev. B **56**, 12847 (1997).

[21] I. Souza, N. Marzari, and D. Vanderbilt, Phys. Rev. B **65**, 035109 (2001).

[22] We used a plane-wave kinetic energy cutoff of 60 Ry and Brillouin-zone coarse grids with 29 irreducible points for the electron-phonon calculation. The electronic energies, phonon frequencies, and electron-phonon matrix elements were interpolated according to Ref. 19 to grids containing 8000 (1000) unique phonon wave vectors and 125 000 (8000) unique electron wave vectors for the rigid-band (supercell) models.

[23] X. Blase, C. Adessi, and D. Connétable, Phys. Rev. Lett. **93**, 237004 (2004).

[24] F. Giustino, Jonathan R. Yates, I. Souza, M. L. Cohen, and G. Louie, Phys. Rev. Lett. **98**, 047005 (2007).

[25] P. Achatz, J. Pernot, C. Marcenat, J. Kacmarcik, G. Ferro, and E. Bustarret, Appl. Phys. Lett. **92**, 072103 (2008).

[26] J. Serrano, J. Strempfer, M. Cardona, M. Schwoerer-Böhning, H. Requardt, M. Lorenzen, B. Stojetz, P. Pavone, and W. J. Choyke, Appl. Phys. Lett. **80**, 4360 (2002).

[27] M. Hoesch, T. Fukuda, J. Mizuki, T. Takenouchi, H. Kawarada, J. P. Sutter, S. Tsutsui, A. Q. R. Baron, M. Nagao, and Y. Takano, Phys. Rev. B **75**, 140508(R) (2007).

[28] L. Boeri, J. Kortus, and O. K. Andersen, Phys. Rev. Lett. **93**, 237002 (2004).

[29] E. Bourgeois and X. Blase, Appl. Phys. Lett. **90**, 142511 (2007).

[30] M. Kriener, Y. Maeno, T. Oguchi, Z.-A. Ren, J. Kato, T. Muranaka, and J. Akimitsu, Phys. Rev. B **78**, 024517 (2008).

[31] K.-W. Lee and W. E. Pickett, Phys. Rev. Lett. **93**, 237003 (2004).

[32] P. B. Allen and B. Mitrovic, in *Solid State Physics*, edited by H. Ehrenreich, F. Seitz, and D. Turnbull, (Academic, New York, 1982), Vol. 32, p. 1.

[33] S. Baroni, S. de Gironcoli, A. Dal Corso, and P. Giannozi, http://www.pwscf.org/.

[34] A. A. Mostofi, J. R. Yates, Y.-S. Lee, I. Souza, D. Vanderbilt, and N. Marzari, Comput. Phys. Commun. **178**, 685 (2008), http://www.wannier.org

[35] E. R. Margine and X. Blase, Appl. Phys. Lett. **93**, 192510 (2008).